Determination of Open Boundary Conditions with an Optimization Method

PETER C. CHU, CHENWU FAN, AND LAURA L. EHRET

Department of Oceanography, Naval Postgraduate School, Monterey, California

23 August 1995 and 8 August 1996

ABSTRACT

The optimization method proposed in this paper is for determining open boundary conditions from interior observations. Unknown open boundary conditions are represented by an open boundary parameter vector (**B**), while known interior observational values are used to form an observation vector (**O**). For a hypothetical **B*** (generally taken as the zero vector for the first time step and as the optimally determined **B** at the previous time step afterward), the numerical ocean model is integrated to obtain solutions (**S***) at interior observation points. The root-mean-square difference between **S*** and **O** might not be minimal. The authors change **B*** with different increments δ**B**. Optimization is used to get the best **B** by minimizing the error between **O** and **S.**

The proposed optimization method can be easily incorporated into any ocean models, whether linear or nonlinear, reversible or irreversible, etc. Applying this method to a primitive equation model with turbulent mixing processes such as the Princeton Ocean Model (POM), an important procedure is to smooth the open boundary parameter vector. If smoothing is not used, POM can only be integrated within a finite period (45 days in this case). If smoothing is used, the model is computationally stable. Furthermore, this optimization method performed well when random noise was added to the ''observational'' points. This indicates that real-time data can be used to inverse the unknown open boundary values.

1. Introduction

One of the difficult problems in shallow-water modeling is the uncertainty of the open boundary condition (OBC). At open boundaries where the numerical grid ends, the fluid motion should be unrestricted. Ideal open boundaries are transparent to motions. Two approaches, local type and inverse type, are available for determining the OBC. The local-type approach determines the OBC from the solution of the governing equations near the boundary. The problem now becomes selection from a set of ad hoc OBCs. Since any ad hoc OBC will introduce inaccuracies into a numerical solution (Chapman 1985), it is important to choose a best one from ad hoc OBCs for a particular ocean model. Using a barotropic coastal ocean model, Chapman (1985) evaluated several of the most used ad hoc OBCs (clamped, sponge, radiation) and found that the best OBC consists of a sponge at the outer edge of the model domain with an Orlanski radiation condition (Orlanski 1976) and that the clamped OBC is probably the worst choice. Applying these results to other ocean models needs further investigation. The local approach suffers drawbacks that may restrict its use: no observational data considered and the ill-posedness of the primitive equations model with ad hoc OBC, that is, it is hard to prove the existence of a unique solution (Bennett 1992; Oliger and Sundstrom 1978). To improve the local approach by using observations at open boundaries, Shulman and Lewis (1995) proposed a method for determining OBCs of the shallow-water model. Their method is based on the integration of governing equations forward in time and the selection of OBCs via a specific inverse problem that minimizes a measure of difference (energy flux) between the values of observed and predicted variables at open boundaries. Thus, their method helps us to select the proper ad hoc OBC by using observations at the open boundaries.

Without any ad hoc OBCs, the inverse-type approach can determine the OBC from a ''best'' fit between model solutions and interior observations. The most popular scheme for this approach is an adjoint method, which consists of four elements: set of control parameters or control vector (e.g., the unknown OBC), numerical ocean model, cost function, and adjoint equation. The cost function is usually defined by the difference between observations and their model counterparts. The adjoint equation is derived from minimizing the cost function with respect to the control parameters. Using an adjoint method, the initial-value problem of ocean model with the OBC becomes integration of both the governing equations and the equation for the control parameters forward and backward in time. For a comprehensive discussion of the adjoint method, the reader is referred to the numerous papers on that subject, for

Corresponding author address: Dr. Peter C. Chu, Naval Postgraduate School, Department of Oceanography, Code OC/CU, Monterey, CA 93943-5000.
E-mail: chu@nps.navy.mil

example, Seiler (1993). The advantage of using the adjoint method is the well posedness and the use of observational data. Seiler (1993) successfully determines the unknown OBCs for a quasigeostrophic ocean by using the adjoint method. The disadvantages that may restrict its use are the requirement of large amounts of computer time and memory; problems of stable integration of the adjoint equation; ocean-model dependency of the adjoint equation; and difficulty in deriving the adjoint equation when the model contains rapidly changing processes, such as ocean mixed layer dynamics.

We propose a simplified method that overcomes the disadvantage of the current inverse-type approach. This method can determine OBCs of *any ocean model* (i.e., a universal method) from interior observations. The essence of the method is to seek the relationship among three vectors: open boundary parameter vector **B**, observation vector **O,** and solution vector **S**. If **B** is given, we can integrate the numerical ocean model and get the solution vector **S**. If **B** is unknown, the optimization method is used to determine **B** by minimizing the root-mean-square (rms) difference between **O** and **S.**

2. Optimization method

a. Three vectors

If r denotes the position of any point along the open boundary Γ, the boundary values of any variable η is a function of r, $\eta^{(b)} = \eta^{(b)}(r)$. Let $f_1(r)$, $f_2(r)$, . . . , $f_n(r)$ be a series of known basis functions. We expand the function $\eta^{(b)}(r)$ into

$$\eta^{(b)}(r) = \sum_{i=1}^{n} b_i f_i(r). \tag{1}$$

Thus, the determination of the open boundary condition $\eta^{(b)}(r)$ becomes the determination of a set of parameters b_1, b_2, . . . , b_n. The n-dimensional vector,

$$\mathbf{B} = \begin{bmatrix} b_1 \\ b_2 \\ \cdot \\ \cdot \\ \cdot \\ b_n \end{bmatrix}, \tag{2}$$

is called the boundary parameter vector.

Assume that there are m observations (O_1, O_2, . . . , O_m) located at the interior (Fig. 1). An m-dimensional vector **O** can be constructed by

$$\mathbf{O} = \begin{bmatrix} O_1 \\ O_2 \\ \cdot \\ \cdot \\ \cdot \\ O_m \end{bmatrix}, \tag{3}$$

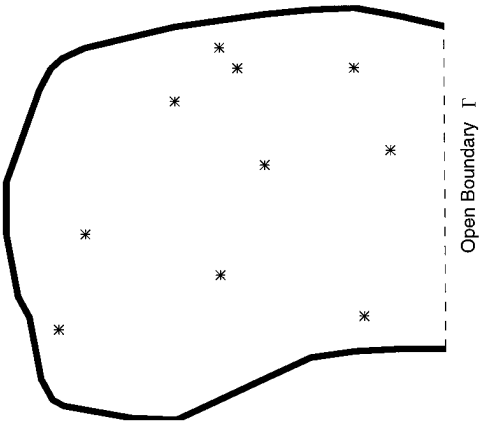

FIG. 1. Can open boundary condition be determined by interior values?

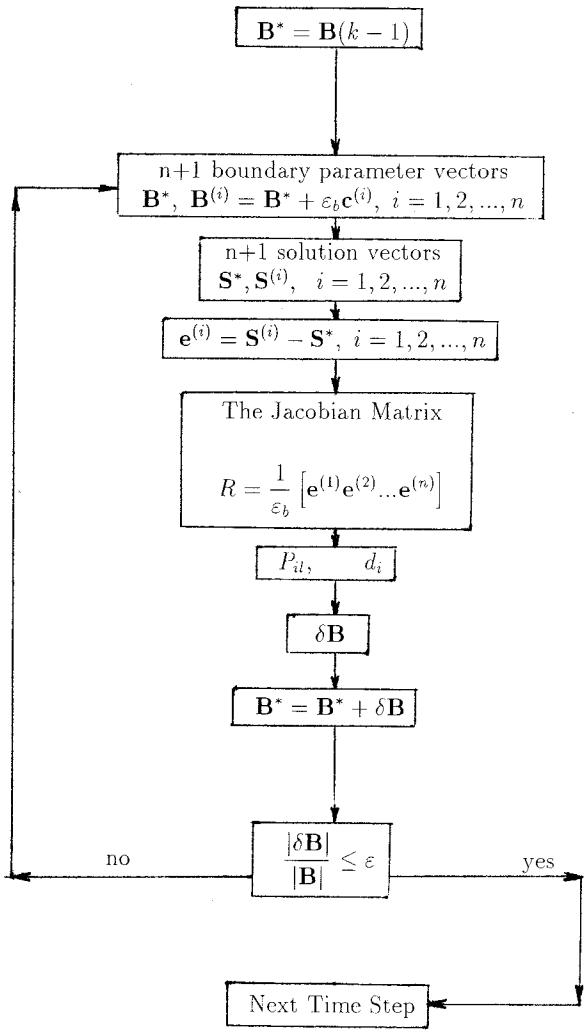

FIG. 2. Flowchart showing the optimization method for determining open boundary vector **B** for the *k*th time step.

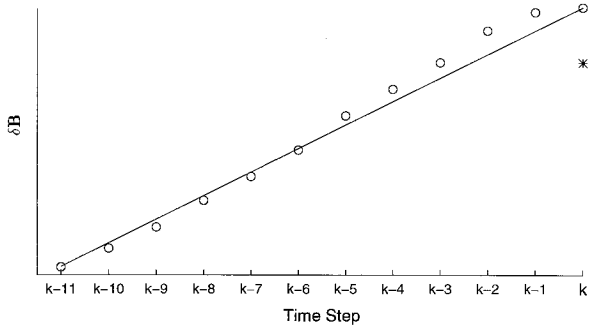

FIG. 3. Smooth of the open boundary correction vector by the linear regression method. Circles indicate smoothed data and asterisks denote unsmoothed data.

which is called the observation vector. Notice that the observational variable is not necessarily the same dimension as the variable at the open boundary. If **B** is given, we can solve the dynamic system and obtain the solution *S.* At the same locations where the observations take place, the solutions are $S_1, S_2, \ldots, S_m$, which form a solution vector

$$\mathbf{S} = \begin{bmatrix} S_1 \\ S_2 \\ \cdot \\ \cdot \\ \cdot \\ S_m \end{bmatrix}. \tag{4}$$

b. Optimization method for determining B

Ocean model performance can be measured by the rms error

$$I = \left[\frac{1}{m} \sum_{j=1}^{m} (S_j - O_j)^2 \right]^{1/2}. \tag{5}$$

The vector **S** depends on **B.** Change of the boundary vector **B** (boundary conditions) leads to a change of **S** (solutions). Inversely, we may determine **B** by minimizing *I*;

$$\frac{\partial I}{\partial b_i} = 0, \qquad i = 1, 2, \ldots, n. \tag{6}$$

Substitution of (5) into (6) leads to a set of n equations implicitly solvable for $b_1, b_2, \ldots, b_n$,

$$\sum_{j=1}^{m} (S_j - O_j) R_{ij} = 0, \qquad i = 1, 2, \ldots, n, \tag{7}$$

where

$$R_{ij} \equiv \frac{\partial S_j}{\partial b_i}; \qquad i = 1, 2, \ldots, n; \qquad j = 1, 2, \ldots, m \tag{8}$$

are components of a $n \times m$ Jacobian matrix $\mathbf{R} = \{R_{ij}\}$.

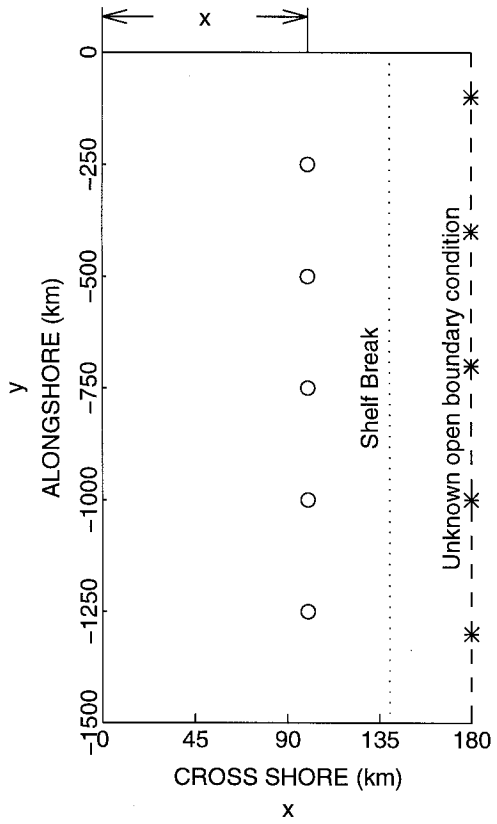

FIG. 4. Integration domain and lateral boundary conditions.

From a first-guess boundary vector **B***, a solution vector **S*** is obtained by solving the numerical ocean model. The rms between **S*** and **O** might not be minimal. We update the boundary parameter vector components by increments $\{\delta b_i \mid i = 1, 2, \ldots, n\}$, and therefore components of the solution vector become

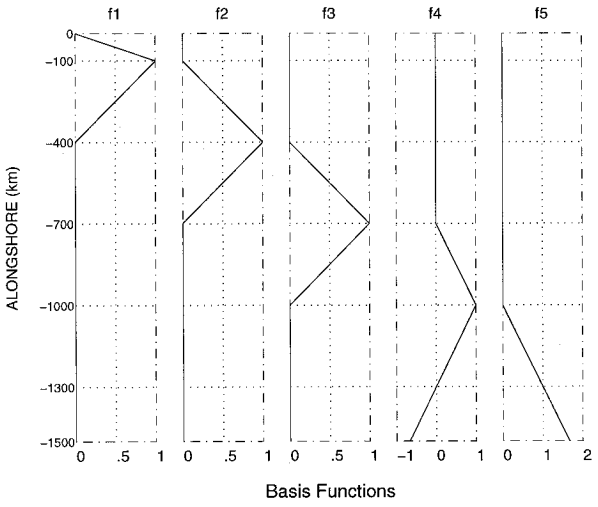

FIG. 5. Five basis functions of the open boundaries, used in the Csanady's shelf model.

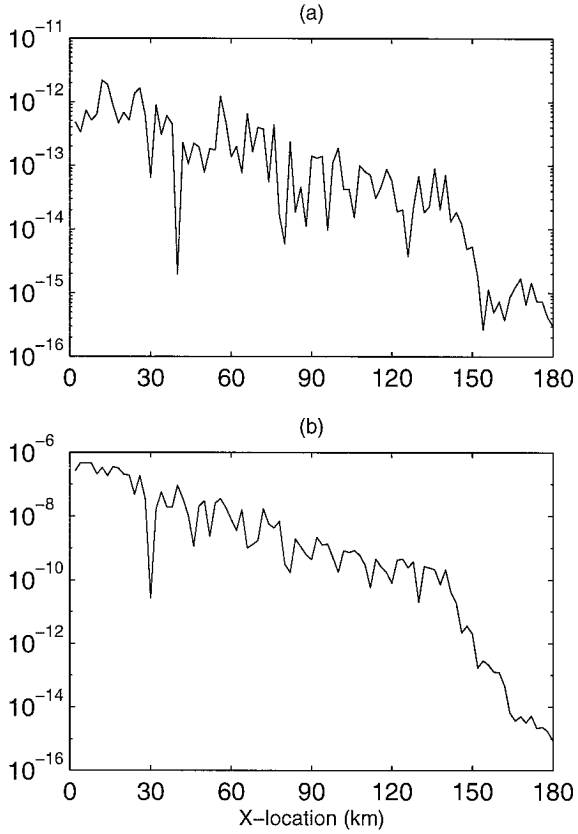

FIG. 6. Sensitivity of relative errors on the cross-coastal location of the observation points: (a) interior error and (b) open boundary error.

$$S_j = S_j^* + \sum_{i=1}^{n} R_{ij}\delta b_i + \text{high-order terms.} \qquad (9)$$

Substituting (9) into (7) and neglecting higher-order terms leads to a set of n linear algebraic equations for $\{\delta b_i\}$,

$$\sum_{l=1}^{n} P_{il}\delta b_l = d_i, \qquad i = 1, 2, \ldots, n, \qquad (10)$$

where

$$P_{il} \equiv \sum_{j=1}^{m} R_{lj}R_{ij}, \qquad d_i \equiv \sum_{j=1}^{m} R_{ij}(O_j - S_j^*); \qquad (11)$$

$$i = 1, 2, \ldots, n; \qquad l = 1, 2, \ldots, n.$$

Both O_j and S^*_j are known quantities. Therefore, the linear algebraic equations (10) have definite solutions when the Jacobian matrix $\{R_{ij}\}$ is determined and

$$\det\{P_{il}\} \neq 0. \qquad (12)$$

c. *Determination of the Jacobian matrix by a multiperturbation method*

As soon as the Jacobian matrix is obtained, we can solve (10) to get boundary parameter vector corrections

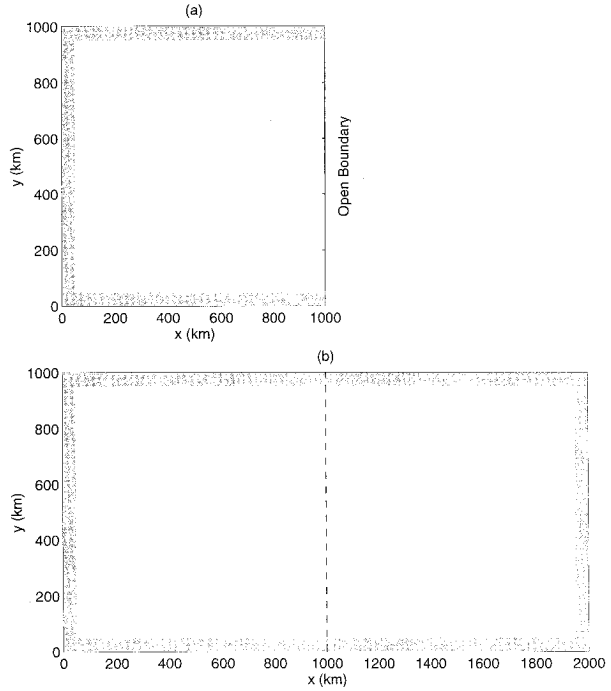

FIG. 7. Two areas for the POM integration: (a) domain with three rigid and one open boundaries and (b) a double size domain with four rigid boundaries.

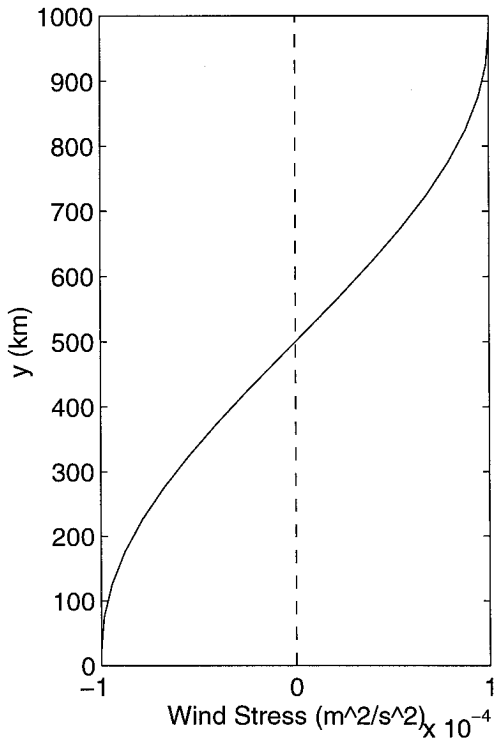

FIG. 8. Pseudo–zonal wind stress ($m^2\ s^{-2}$) used in the POM integration.

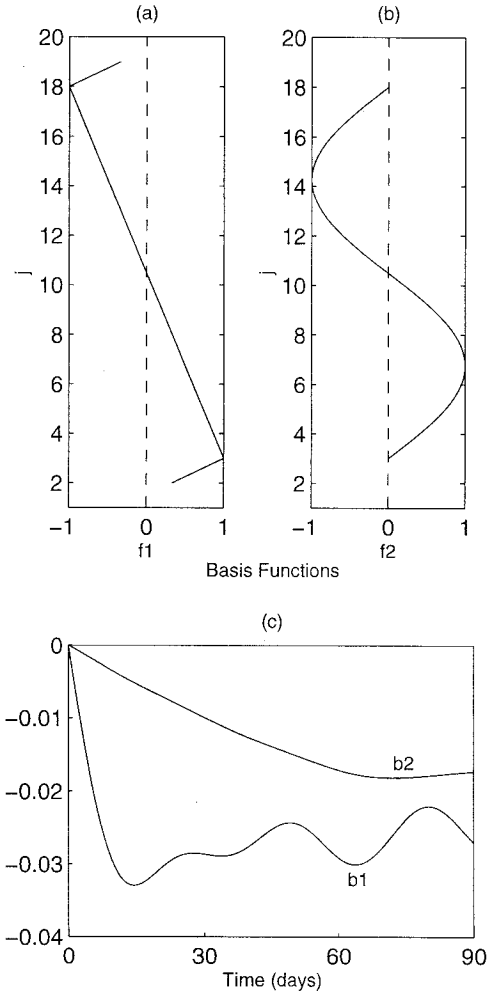

FIG. 9. Basis functions and corresponding amplitudes: (a) $f_1(y)$, (b) $f_2(y)$, and (c) $b_1(t)$ and $b_2(t)$.

δbi ($i = 1, 2, \ldots, n$). Therefore, the determination of the Jacobian matrix is the key issue. We propose a simple multiperturbation method on the first-guess boundary parameter vector $\mathbf{B}^*$ to get the Jacobian matrix. The vector $\mathbf{B}^*$ at the initial state ($t = 0$) of any numerical ocean model is set to be a zero vector,

$$\mathbf{B}^*(0) = \begin{bmatrix} 0 \\ 0 \\ \cdot \\ \cdot \\ \cdot \\ 0 \end{bmatrix}, \tag{13}$$

and the first guess for $\mathbf{B}$ at time step k is set to be the same as the determined boundary parameter vector at time step $k - 1$,

$$\mathbf{B}^*(k) = \mathbf{B}(k - 1), \qquad k = 1, 2, \ldots. \tag{14}$$

We define a set of n-dimensional unit vectors

$$\mathbf{c}^{(1)} = \begin{bmatrix} 1 \\ 0 \\ 0 \\ \cdot \\ \cdot \\ 0 \end{bmatrix}, \qquad \mathbf{c}^{(2)} = \begin{bmatrix} 0 \\ 1 \\ 0 \\ \cdot \\ \cdot \\ 0 \end{bmatrix}, \ldots, \qquad \mathbf{c}^{(n)} = \begin{bmatrix} 0 \\ 0 \\ 0 \\ \cdot \\ \cdot \\ 1 \end{bmatrix} \tag{15}$$

and perturb the first guess at each time step by a small fraction of these unit vectors $\mathbf{c}^{(i)}$:

$$\mathbf{B}^{(i)} = \mathbf{B}^* + \epsilon_b \mathbf{c}^{(i)}, \qquad i = 1, 2, \ldots, n, \tag{16}$$

where ϵ_b is a small positive number. Using the $n + 1$ sets of boundary parameter vectors $\mathbf{B}^*$, $\mathbf{B}^{(1)}$, $\mathbf{B}^{(2)}$, ..., $\mathbf{B}^{(n)}$, we obtain $n + 1$ sets of solution vectors for that time step, $\mathbf{S}^*$, $\mathbf{S}^{(1)}$, $\mathbf{S}^{(2)}$, ..., $\mathbf{S}^{(n)}$. The Jacobian matrix (8) denotes the rate of change of the solution vector with the boundary parameter vector; therefore, it can be computed by

$$R = \frac{1}{\epsilon_b}[\mathbf{e}^{(1)}\mathbf{e}^{(2)} \cdots \mathbf{e}^{(n)}], \tag{17}$$

where the m-dimensional vectors $\mathbf{e}^{(1)}$, $\mathbf{e}^{(2)}$, ..., $\mathbf{e}^{(n)}$ are defined by

$$\mathbf{e}^{(i)} \equiv \mathbf{S}^{(i)} - \mathbf{S}^*, \qquad i = 1, 2, \ldots, n. \tag{18}$$

d. Iteration process

After the algebraic equation (10) is solved, the boundary parameter correction vector $\delta\mathbf{B} \equiv (\delta b_1, \delta b_2, \ldots, \delta b_n)$ is obtained. We replace $\mathbf{B}^*$ by $\mathbf{B}^* + \delta\mathbf{B}$ and repeat the process (Fig. 2) until reaching a certain criterion

$$\frac{|\delta\mathbf{B}|}{|\mathbf{B}^*|} \le \epsilon,$$

where

$$|\mathbf{B}^*| \equiv \left(\frac{1}{n}\sum_{i=1}^{n} b_i^2\right)^{1/2}, \qquad |\delta\mathbf{B}| \equiv \left(\frac{1}{n}\sum_{i=1}^{n} \delta b_i^2\right)^{1/2}, \tag{19}$$

and ϵ is a small positive number (user input). As soon as the inequality (19) is satisfied, the iteration stops and the final $\mathbf{B}^*$ becomes the optimal boundary parameter vector for the next time step.

e. Reference model

A model with a given boundary condition (called reference boundary condition) is needed for error estimation. We run the model with the given reference boundary condition and obtain the solution for interior points, $\mathbf{O} = (O_1, O_2, \ldots, O_m)$, which are taken as ''observations.'' We also expand the reference boundary values into basis functions (1) to obtain the reference boundary vector $\mathbf{B}^{(\mathrm{ref})} = (b_1^{\mathrm{ref}}, b_2^{\mathrm{ref}}, \ldots, b_n^{\mathrm{ref}})$. Such a model (with known boundary conditions) is called a reference model.

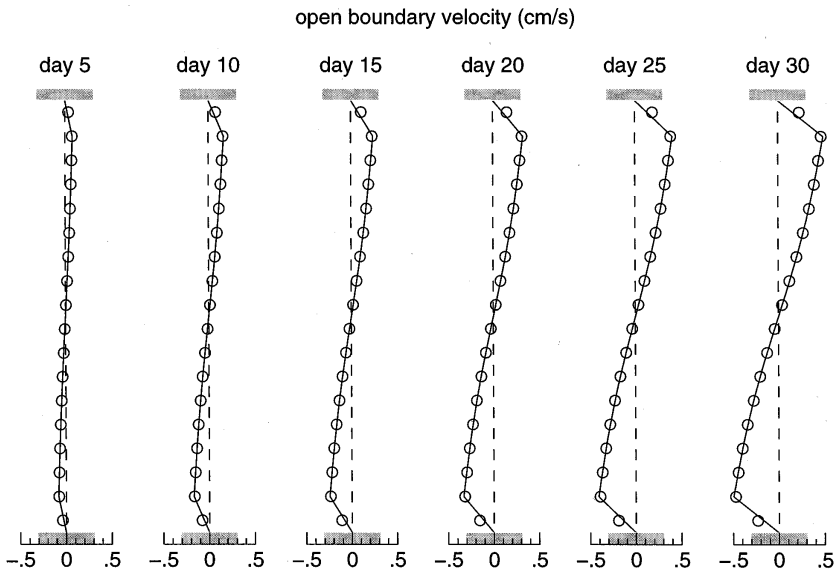

FIG. 10. Time series of open boundary values of the domain A. The dots represent the values computed from the basis functions.

f. Smoothing δB

Both observational (instrument) and computational (numerical) errors perturb the values of **B**. When the reference model results are used, there is no instrument error in observations. But the computational errors still cause errors in **B**. For prognostic ocean models, the errors of **B** feed back to the next step model integration. Error accumulation in each time step may cause computational instability. We use linear regression for smoothing $\delta\mathbf{B}$ to reduce high-frequency modes. The procedure is as follows: 1) For the first 11 time steps, we do not do any smoothing, and after the 11th time step, we use the smoothing technique. 2) For each time step k ($k > 11$), we maintain smoothed values of each component at the previous 11 steps, $\delta b_j^{(s)}(k-11)$, $\delta b_j^{(s)}(k-10)$, . . . , $\delta b_j^{(s)}(k-1)$. Here the superscript s indicates smoothed value. 3) We fit a linear regression to fit the 12 values: $\delta b_j^{(s)}(k-11)$, $\delta b_j^{(s)}(k-10)$, . . . , $\delta b_j^{(s)}(k-1)$, and $\delta b_j(k)$. 4) We obtain the value at the time step k from the regression, $\delta b_j^{(s)}(k)$. 5) We replace $\delta b_j(k)$ by $\delta b_j^{(s)}(k)$. Such a treatment (Fig. 3) will filter out high-frequency noise in the derived open boundary parameter vector.

g. Random noises added on ''observations''

When observations are taken from the reference model solution, there is no observational (instrument) error. In order to see the effects of observational error on the determination of open boundary conditions, we add a Gaussian-type random variable to each observation at each time step. The probability distribution function is given by

$$F(\delta O) = \frac{1}{\sqrt{2\pi}\sigma}\exp\left[-\frac{(\delta O)^2}{2\sigma^2}\right], \tag{20}$$

where δO is a random variable with a zero mean and a standard deviation of σ.

h. Relative errors

For a given observation vector **O** and unknown open boundary condition, we use the optimization method to obtain the values at the open boundary, $\mathbf{B} = (b_1, b_2, \ldots, b_n)$. Then we integrate the same model with the computed open boundary condition and get the solutions at the observational points, $\mathbf{S} = (S_1, S_2, \ldots, S_m)$. The relative errors,

$$E^{(B)} \equiv \frac{\sum |b_i^{\text{ref}} - b_i|}{\sum |b_i^{\text{ref}}|}, \qquad E^{(O)} \equiv \frac{\sum |O_j - S_j|}{\sum |O_j|}, \tag{21}$$

measure the validity of the optimization method. The smaller the $E^{(B)}$ and $E^{(O)}$, the better the optimization method.

3. Linear ocean models

a. Jacobian matrix

For any linear ocean model, the relationship between $\{S_j\}$ and $\{\delta b_i\}$ becomes linear. There are no high order terms in (9). The Jacobian matrix can be easily obtained by letting

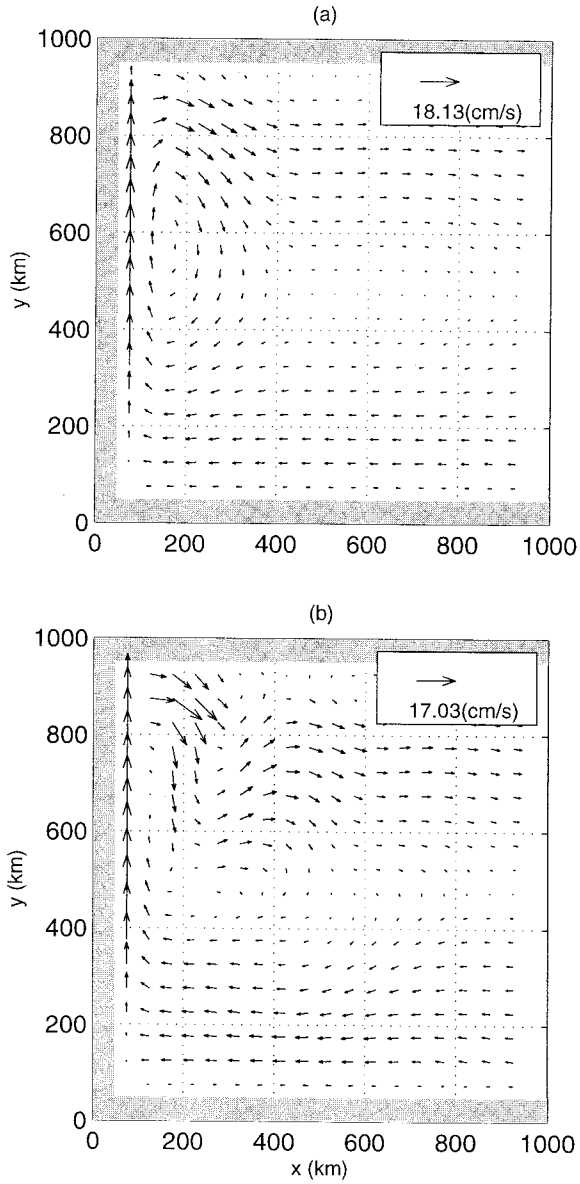

FIG. 11. The velocity fields from the reference model results after (a) 30 day's run and (b) 90 day's run.

$$\mathbf{B}^* = \begin{bmatrix} 0 \\ 0 \\ \cdot \\ \cdot \\ \cdot \\ 0 \end{bmatrix}, \qquad \epsilon_b = 1,$$

for any time step. The algebraic equation (9) becomes

$$R\mathbf{B}^{(i)} = \mathbf{e}^{(i)} \qquad i = 1, 2, \ldots, n.$$

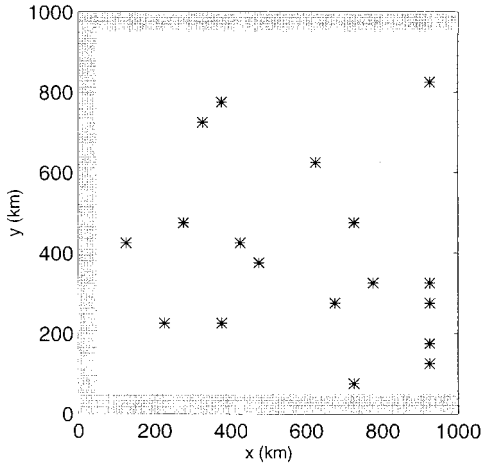

FIG. 12. Randomly picked observational points for the POM model.

b. *Example—Csanady's shelf model*

We use a steady-state shelf circulation model proposed by Csanady (1978) as an example to show how to obtain the Jacobian matrix **R** and to determine the open boundary conditions. Consider a long and straight coastline with coordinates such that the y axis coincides with the coast and positive x points offshore. The water depth is a function only of offshore distance, that is, $h = h(x)$. As pointed out by Csanady (1978), this model is appropriate for simulating mean flow along such a coast driven by mean wind stress.

Under the assumptions of homogeneous water and linear bottom friction (i.e., proportional to depth-averaged velocity), the dynamical equations for depth-averaged velocities (u, v) without wind forcing become

$$-fv = -g\frac{\partial \eta}{\partial x} \tag{22}$$

$$fu = -g\frac{\partial \eta}{\partial y} - \frac{rv}{h} \tag{23}$$

$$\frac{\partial (uh)}{\partial x} + \frac{\partial (vh)}{\partial y} = 0, \tag{24}$$

where η is the surface elevation, r the bottom resistance coefficient, f the Coriolis parameter, and g the gravity. Eliminating u and v from (22)–(24) leads to a single equation for the surface elevation η:

$$\frac{\partial^2 \eta}{\partial x^2} + \frac{f}{r}\frac{dh}{dx}\frac{\partial \eta}{\partial y} = 0. \tag{25}$$

Wang (1982) applied the Csanady model to a region (Fig. 4) with a combined flat shelf and steep slope, depicted by

$$h(x) = \begin{cases} 0.02 + 10^{-3}x, & 0 \le x \le x_0 \\ 0.16 + 0.05(x - x_0), & x_0 \le x \le x_1, \\ 2.0, & x > x_1, \end{cases}$$

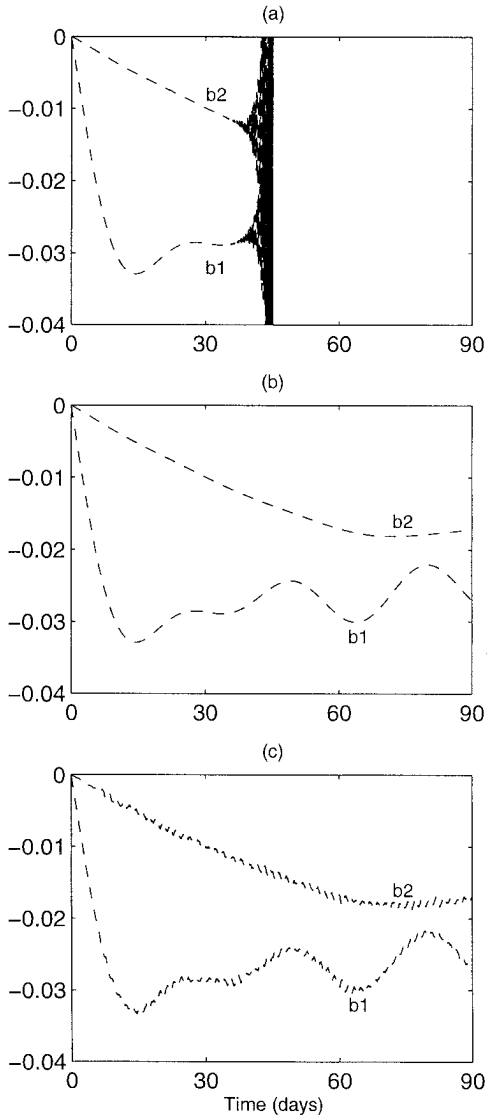

FIG. 13. Components of the open boundary parameter vector obtained by the optimization method for (a) case 1, (b) case 2, and (c) case 3.

where $x_0 = 140$ km and $x_1 = 180$ km are the offshore location of the shelf break and slope edge, respectively. Following Wang (1982), we chose $f = 10^{-4}$ s^{-1}, and $r = 0.1$ cm s^{-1}, and use the boundary condition at the coast ($x = 0$),

$$\frac{\partial \eta}{\partial y} + \frac{r}{fh(x_0)}\frac{\partial \eta}{\partial x} = 0. \tag{26}$$

We consider the pure open ocean forcing case; that is, there is no inflow at the backward boundary ($y = 0$),

$$\eta = 0, \text{ at } y = 0. \tag{27}$$

Equation (25) has the form of the one-dimensional heat-conduction equation, with negative y playing the role of time. We solve (25) numerically by the Gaussian elimination method under the boundary conditions (26)–(27) to obtain the first-guess solution at the interior. The spatial increments are $\Delta x = 2$ km, $\Delta y = 10$ km. We use the five basis functions $f_1(y)$, $f_2(y)$, . . . , $f_5(y)$ (Fig. 5) for $\eta^{(b)}$. The first guess for $\mathbf{B}$ is the zero vector. For simplicity and no loss of generality, we choose five equally spaced points on an interior line paralleling to the y axis as observation points. In this case,

$$[\mathbf{B}^{(1)}\mathbf{B}^{(2)}\cdots\mathbf{B}^{(5)}] = \begin{bmatrix} 1 & 0 & 0 & 0 & 0 \\ 0 & 1 & 0 & 0 & 0 \\ 0 & 0 & 1 & 0 & 0 \\ 0 & 0 & 0 & 1 & 0 \\ 0 & 0 & 0 & 0 & 1 \end{bmatrix} \tag{28}$$

is a unit matrix. The Jacobian matrix then becomes

$$\mathbf{R} = [\mathbf{e}^{(1)}\mathbf{e}^{(2)}\mathbf{e}^{(3)}\mathbf{e}^{(4)}\mathbf{e}^{(5)}]. \tag{29}$$

c. Error estimation

For simplicity, we choose Wang's (1982) solution along with the open boundary condition as a reference model for the error estimation. Five observation points are equally spaced and located along lines paralleling to the y axis. These lines are represented by their x coordinate. Wang's (1982) solution at the five points is taken as observations, $\mathbf{O} = (O_1, O_2, O_3, O_4, O_5)$, and the Wang's open boundary vector is denoted by $\mathbf{B}^{(\text{ref})} = (b_1^{\text{ref}}, b_2^{\text{ref}}, b_3^{\text{ref}}, b_4^{\text{ref}}, b_5^{\text{ref}})$. Since the model is steady state, we did not smooth $\delta\mathbf{B}$.

The five observation points are given as $\mathbf{O}$ with unknown open boundary condition. Using the optimization method, we obtain values at the open boundary, $\mathbf{B} = (b_1, b_2, b_3, b_4, b_5)$. Then, we integrate the Csanady model (24) with the computed open boundary condition, and get the solutions at the same five points, $\mathbf{S} = (S_1, S_2, S_3, S_4, S_5)$. Since the observation points are on the lines paralleling the y axis in this study, $E^{(B)}$ and $E^{(O)}$ depend only on x. Surprisingly, both $E^{(B)}$ and $E^{(O)}$ are extremely small (Fig. 6). When the observation points are chosen near the coast, the relative errors are on the order of 10^{-6}–10^{-7}. At the shelf break ($x = x_0$, $x_0 = 140$ km), $E^{(B)}$ is on the order of 10^{-6}. Passing the shelf break, $E^{(B)}$ and $E^{(O)}$ decrease very fast offshore and are on the order of 10^{-16} near the open boundary.

4. Nonlinear ocean model

a. Example—Princeton Ocean Model (POM)

We apply the optimization method to determine the open boundary conditions of a flat bay centered at 35°N and bounded by three rigid boundaries. This bay expands 1000 km in both the north–south and east–west directions. The northern, southern, and western boundaries are rigid, and the eastern boundary is open. The

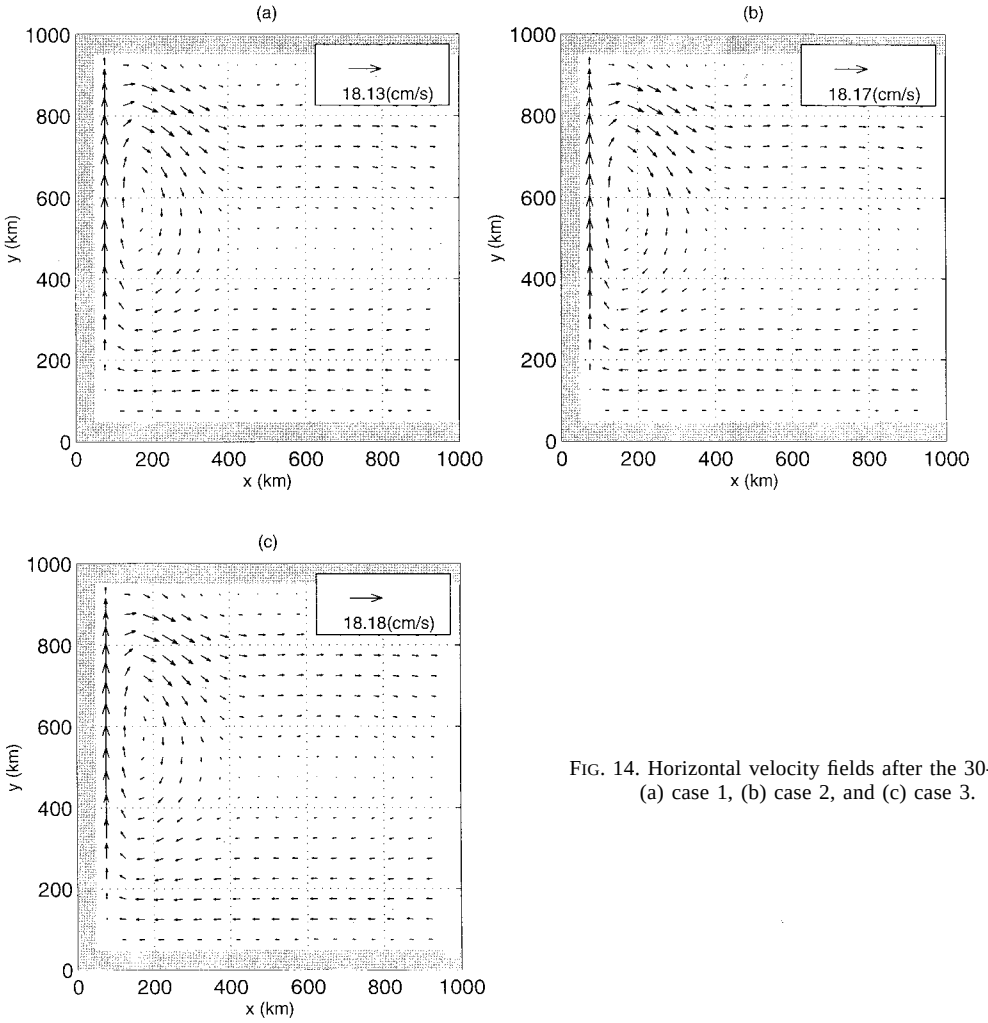

FIG. 14. Horizontal velocity fields after the 30-day run: (a) case 1, (b) case 2, and (c) case 3.

Cartesian coordinate system is chosen with the origin at the southwest corner. The x axis points toward the east, and the y axis toward the north (Fig. 7a). The circulation in the bay is modeled with the Princeton Ocean Model (POM) developed by Blumberg and Mellor (1987). POM is a primitive equation model with a free surface and a level-2 turbulence closure scheme (Mellor and Yamada 1982). A description of the model code can be found in Mellor (1991). We use the 2D version of POM to illustrate the usefulness of the optimization method for determining the open boundary conditions.

The area depicted in Fig. 7a is called domain A, where the boundary conditions are known at the three rigid boundaries (northern, southern, and western), and unknown at the eastern boundary. The eastern boundary of domain A is connected to a mirror image of domain A (about $x = 1000$ km) forming a closed rectangular domain (Fig. 7b), called domain B. The POM model was integrated from the following initial conditions,

$$(u, v, w) = 0 \text{ (m s}^{-1}\text{)}, \quad T = 283(1 + e^{z/1000}) \text{ (K)},$$
$$S = 35 \qquad \text{(psu)}, \tag{30}$$

under no surface heat or salinity fluxes and zonal surface pseudo–wind stress varying with latitude (Fig. 8):

$$\frac{\tau_x}{\rho_0} = -10^{-4} \cos\frac{\pi y}{L_y} \qquad (\text{m}^2\ \text{s}^{-2}). \tag{31}$$

The time step was chosen as 2 min. The horizontal resolution was 50 km. Bottom stress is parameterized by the quadratic drag relation. Horizontal kinematic viscosity is set to be 500 $\text{m}^2\ \text{s}^{-1}$.

b. Boundary vector

We integrate POM over domain B with four rigid boundaries (known boundary conditions) from the initial conditions (30) and surface forcing (31) and take the solution along the middle of domain B ($x = 1000$ km) as the reference open boundary condition for the

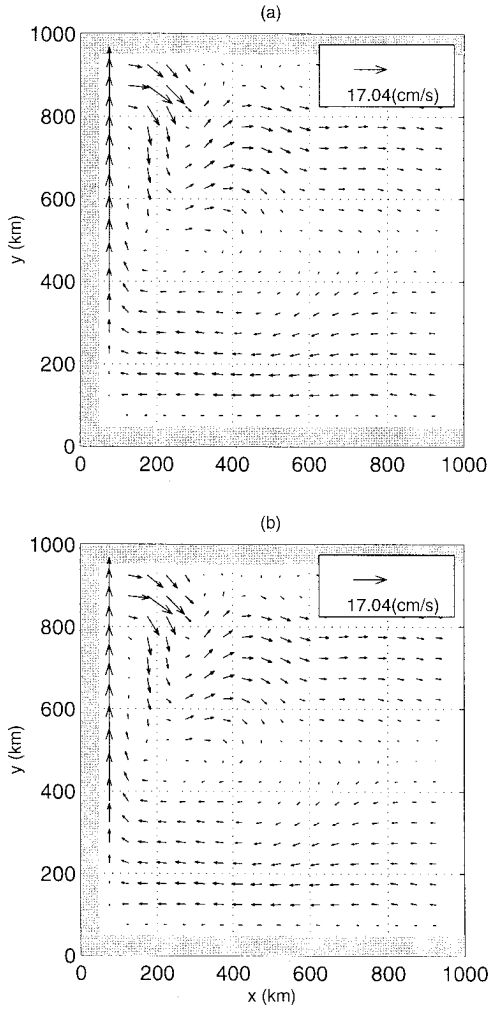

FIG. 15. Horizontal velocity fields after the 90 day's run: (a) case 2 and (b) case 3.

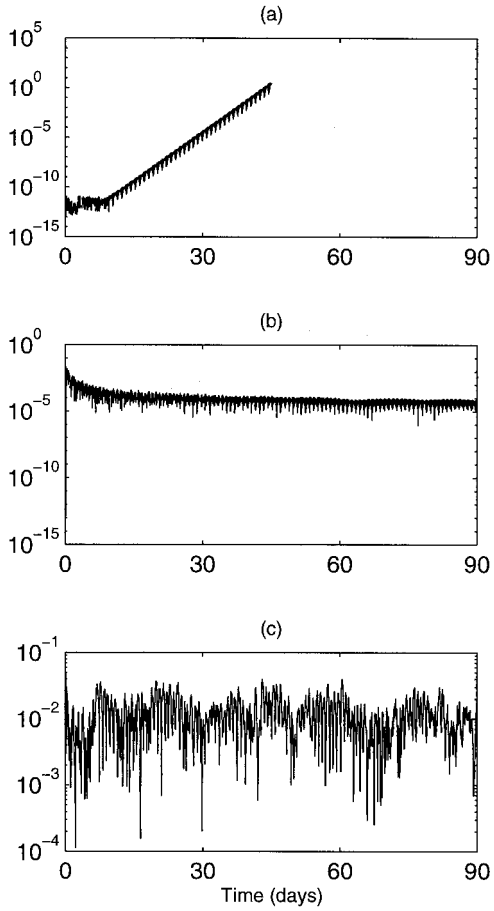

FIG. 16. The relative boundary vector error for (a) case 1, (b) case 2, and (c) case 3.

domain A integration. The velocity at $x = 1000$ km for the domain B run is nearly zonal,

$$|v| \ll |u| \text{ at } x = 1000 \text{ km}.$$

For simplicity and no loss of generality, we assume zero latitudinal velocity at the eastern open boundary for the domain A integration. Therefore, our task here is to determine the zonal velocity at the eastern open boundary. Following the procedure depicted in section 2, we expand the boundary values by two basis functions $f_1(y)$ and $f_2(y)$ (Figs. 9a,b),

$$u^{(b)}(y, t) = b_1(t)f_1(y) + b_2(t)f_2(y) \tag{32}$$

with two temporally varying amplitudes $b_1(t)$ and $b_2(t)$, as shown in Fig. 9c. After plotting the time series (from day 5 to day 30) of the reference open boundary values and the corresponding expanded values (Fig. 10), we find that the boundary parameters can be well represented by the two-dimensional vector,

$$\mathbf{B}(t) = [b_1(t), b_2(t)]. \tag{33}$$

c. Reference model

We choose the POM model solution for domain A computed with the reference open boundary condition determined by the two time series $b_1(t)$, $b_2(t)$ (Fig. 9) as a reference model. We ran the reference model for 90 days with known boundary conditions (three rigid and one reference open boundary condition). Figure 11 shows the horizontal velocity of the reference model run for two different times (30 day and 90 day). We will use the reference model results to verify the optimization method.

d. Three cases

A random number generator (Fortran function, Ranf) was used to produce random disturbances for each observational point independently with mean value of zero and standard deviation of 0.01 m s^{-1}. In order to test the performance of the optimization method, we ran three cases: 1) without smoothing on $\delta\mathbf{B}$ and without

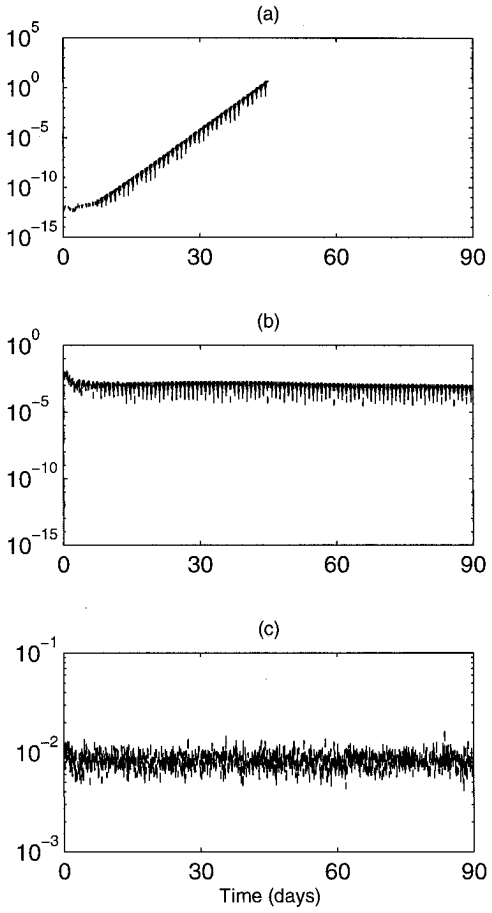

FIG. 17. The relative error at the observational points for (a) case 1, (b) case 2, and (c) case 3.

random noise added to the observations, 2) with smoothing on $\delta\mathbf{B}$ and without random noise added to the observations, and 3) with both smoothing on $\delta\mathbf{B}$ and random noise added to the observations.

Eighteen randomly picked points are treated as observational points (Fig. 12). The reference model solution at the 18 points is the observations, $\mathbf{O} = (O_1, O_2, \ldots, O_{18})$. Using the optimization method, we obtain the temporally varying $b_1(t)$ and $b_2(t)$ for the three cases. For case 1 (Fig. 13a), both b_1 and b_2 fit the reference values (Fig. 9c) very well until the 35th day. After that day, b_1 and b_2 change rapidly with time and finally blow up at the 45th day. For case 2 (Fig. 13b), both b_1 and b_2 fit the reference values (Fig. 9c) very well. For case 3 (Fig. 13c), both b_1 and b_2 are very close to the reference values (Fig. 9c) with small perturbations. Figure 13 tells us that smoothing on $\delta\mathbf{B}$ is a key issue for this method.

We integrate the POM for domain A with the computed open boundary conditions from b_1 and b_2 for the three cases. The 30th day's horizontal velocity fields (Fig. 14) for the three cases all agree quite well with the reference model results (Fig. 11a), and the 90th day's horizontal velocity fields (Fig. 15) for cases 2 and 3 agree quite well with the reference model results (Fig. 11b).

e. Error estimation

Similar to the linear case, we use 18 interior observations $\mathbf{O}$, the reference boundary vector $\mathbf{B}^{\text{ref}} = (b_1^{\text{ref}}, b_2^{\text{ref}})$, the open boundary vector $\mathbf{B} = (b_1, b_2)$, and the interior solution $\mathbf{S} = (S_1, S_2, \ldots, S_{18})$ for error estimation.

The boundary errors $E^{(B)}$ for the three cases are shown in Fig. 16. When there is no smoothing on $\delta\mathbf{B}$ (case 1), $E^{(B)}$ keeps very small values (10^{-12}–10^{-13}) for the first few days. After the eighth day, $E^{(B)}$ increases exponentially with time and reaches the order of 1 at the 45th day. This indicates that we cannot use the optimization method without smoothing on $\delta\mathbf{B}$. When there is smoothing on $\delta\mathbf{B}$ and no noise added to the observations (case 2), $E^{(B)}$ has larger values ($\sim 10^{-2}$) than case 1 at the beginning, then rapidly decreases with time during the first 10 days and gradually decreases with time afterward. After 10 days of integration, the magnitude of $E^{(B)}$ is on the order of 10^{-4}–10^{-5}. When there is smoothing on $\delta\mathbf{B}$ and noise added to the observations (case 3), $E^{(B)}$ fluctuates around $10^{-2.5}$ ($\simeq 3.162 \times 10^{-3}$) with the maximum value near $10^{-1.5}$ ($\simeq 0.03$) and the minimum value around 10^{-4}. Figure 16 indicates that smoothing on $\delta\mathbf{B}$ is very important for this method.

The interior errors $E^{(O)}$ for the three cases are shown in Fig. 17. When there is no smoothing on $\delta\mathbf{B}$ (case 1), $E^{(O)}$ keeps very small values (10^{-13}) for the first few days and then increases exponentially with time and reaches the order of 1 at the 45th day. When there is smoothing on $\delta\mathbf{B}$ and no noise added to the observations (case 2), $E^{(O)}$ has larger values ($\sim 10^{-2}$) than case 1 at the beginning then rapidly decreases with time during first 10 days and gradually decreases with time afterward. After 10 days of integration, the magnitude of $E^{(O)}$ is on the order of 10^{-4}–10^{-5}. When there is smoothing on $\delta\mathbf{B}$ and noise added to the observations (case 3), $E^{(O)}$ fluctuates around $10^{-2.2}$ ($\simeq 6.3 \times 10^{-3}$) with the maximum value near 10^{-2} and the minimum value around $10^{-2.4}$ ($\simeq 3.9 \times 10^{-3}$). Both Figs. 16 and 17 indicate that smoothing on $\delta\mathbf{B}$ is very important for determining open boundary conditions.

5. Conclusions

1) The proposed optimization method provides a useful scheme to obtain unknown open boundary values from known interior values. Different from the adjoint method, this scheme can be easily incorporated into any ocean models.
2) Extremely small computational errors are found in applying this method to the Csanady shelf model, which proves the feasibility of using this optimization method for linear models.

3) For time-dependent dynamical models, when the temporally varying values are given at interior observation points, the optimization method can be used for each time step to obtain the unknown open boundary values for that time step.
4) For a primitive equation model with turbulent mixing processes (e.g., POM), it is very important to use smoothing on the open boundary parameter vector. If smoothing is not used, POM can be integrated only within a certain period (45 days in our case) and will blow up afterward. If smoothing is used, the model is computationally stable.
5) This optimization method performs well even when random noises are added to the observational points (case 3). This indicates that we can use real-time data to invert for the unknown open boundary values.

Acknowledgments. This research is sponsored by the Office of Naval Research (ONR) Naval Ocean Modeling and Prediction (NOMP) Program and the Naval Postgraduate School.

REFERENCES

Bennett, A., 1992: *Inverse Methods in Physical Oceanography*. Cambridge University Press, 346 pp.

Blumberg, A. F., and G. L. Mellor, 1987: A description of a three-dimensional coastal ocean circulation model. *Three Dimensional Coastal Ocean Models*, N. S. Heaper, Ed., Amer. Geophys. Union, 1–16.

Chapman, D., 1985: Numerical treatment of cross-shelf open boundaries in a barotropic ocean model. *J. Phys. Oceanogr.*, **15,** 1060–1075.

Csanady, G. T., 1978: The arrested topographic waves. *J. Phys. Oceanogr.*, **8,** 47–62.

Mellor, G. L., 1991: *User's Guide for a Three Dimensional, Primitive Equation, Numerical Ocean Model.* Princeton University.

——, and T. Yamada, 1982: Development of a turbulence closure model for geophysical fluid problems. *Rev. Geophys. Space Phys.*, **20** (4), 851–875.

Oliger, J., and A. Sundstrom, 1978: Theoretical and practical aspects of some initial boundary value problems in fluid dynamics. *SIAM J. Appl. Math*, **35** (3), 419–446.

Orlanski, I., 1976: A simple boundary condition for unbounded hyperbolic flows. *J. Comput. Phys.*, **21,** 251–269.

Seiler, U., 1993: Estimation of the open boundary conditions with the adjoint method. *J. Geophys. Res.*, **98** (C12), 22 855–22 870.

Shulman, I., and J. K. Lewis, 1995: Optimization approach to the treatment of open boundary conditions. *J. Phys. Oceanogr.*, **25,** 1006–1011.

Wang, D. P., 1982: Effects of continental slope on the mean shelf circulation. *J. Phys. Oceanogr.*, **12,** 1524–1526.